PHILOSOPHICAL TRANSACTIONS B

royalsocietypublishing.org/journal/rstb

Research

Cite this article: Zeng B, Zhang X, Schimpf R, Powers A, Glikson M, Antzelevitch C, Hu D, Barajas-Martinez H. 2023 Functional identification of hot-spot mutations in cardiac calcium channel genes associated with the J wave syndromes. *Phil. Trans. R. Soc. B* **378**: 20220286.
https://doi.org/10.1098/rstb.2022.0286

Received: 14 October 2022
Accepted: 22 March 2023

One contribution of 23 to a theme issue 'The heartbeat: its molecular basis and physiological mechanisms'.

Subject Areas:
genetics, biophysics, physiology

Keywords:
Brugada syndrome, early repolarization syndrome, genetics, electrophysiology, sudden cardiac death

Authors for correspondence:
Dan Hu
e-mails: hudan0716@hotmail.com, rm002646@whu.edu.cn
Hector Barajas-Martinez
e-mail: barajash69@hotmail.com

†These authors contribute equally to this work as the first authors.

THE ROYAL SOCIETY PUBLISHING

Functional identification of hot-spot mutations in cardiac calcium channel genes associated with the J wave syndromes

Bin Zeng[1,2,†], Xiang Zhang[1,2], Rainer Schimpf[3], Andrew Powers[4], Michael Glikson[5], Charles Antzelevitch[6,7], Dan Hu[1,2,†] and Hector Barajas-Martinez[1,2,6,7]

[1]Department of Cardiology and Cardiovascular Research Institute, Renmin Hospital of Wuhan University, Wuhan, Hubei, 430060, People's Republic of China
[2]Hubei Key Laboratory of Cardiology, Renmin Hospital of Wuhan University, Wuhan, Hubei, 430060, People's Republic of China
[3]Cardiology Practice Clinic, Ludwig-Guttmann-Str. 11, Ludwigshafen, Ludwigshafen-Neustadt, 67071, Germany
[4]Department of Biology, University at Albany, State University of New York, Albany, NY, 12222, USA
[5]Jesselson Integrated Heart Center, Shaare Zedek Medical Center and Hebrew University Faculty of Medicine, Jerusalem, 91031, Israel
[6]Lankenau Institute for Medical Research, and Lankenau Heart Institute, Wynnwood, Pennsylvania, PA, 19096, USA
[7]Sidney Kimmel Medical College, Thomas Jefferson University, Philadelphia, PA, 19107, USA

XZ, 0000-0001-9494-6064; DH, 0000-0002-0994-8434

J wave syndrome (JWS) is an inherited cardiac channelopathy associated with malignant ventricular arrhythmias and sudden cardiac death (SCD), which comprises early repolarization syndrome and Brugada syndrome. Here, we explore the association between variants in the *L*-type calcium channel gene subunits, α_{1C} (*CACNA1C*) and β2b (*CACNB2b*), and the JWS phenotype. Using next-generation genetic sequencing of 402 JWS probands and their family members, we identified a *CACNA1C*-G37R (p.Gly37Arg) mutation in five individuals in four families, two of which had a family history of SCD as well as a *CACNB2b*-S143F (p.Ser143Phe) mutation in seven individuals in three families, two of which had a family history of SCD. The variants were located in exon 2 in *CACNA1C* and exon 5 in *CACNB2b*; both were in highly conserved amino acid residues. Whole-cell patch-clamp results showed that compared with the wild-type group, calcium current density of *CACNB2b*-S143F and *CACNA1C*-G37R were significantly lower displaying a dominant-negative effect. Our findings provide further support for the hypothesis that variants in *CACNA1C* and *CACNB2b* are associated with JWS. The results suggest that mutations in these two genes lead to loss-of-function of the cardiac calcium channel current warranting their inclusion in genetic screening protocols.

This article is part of the theme issue 'The heartbeat: its molecular basis and physiological mechanisms'.

1. Introduction

In recent years, the J wave and J wave syndrome (JWS) have received much attention because of its association with life-threatening ventricular arrhythmias and sudden cardiac death (SCD), the latter is comprised of Brugada syndrome (BrS) and early repolarization syndrome (ERS) [1]. SCD has been recognized as one of the leading causes of death accounting for up to 20% of all-cause deaths in developed countries, with an annual toll of about 50–100/100 000 people [2,3]. In BrS, three ECG patterns are recognized. The ECG pattern diagnostic of BrS is a Type 1 ST-segment elevation characterized by a coved-type ST-segment

elevation in the right precordial leads (V1–V3). A Type 2 BrS pattern is characterized by a 'saddle-back' configuration with an ST-segment elevation of greater than or equal to 1 mm in right precordial leads, whereas a Type 3 is characterized by a similar shape with ST-segment elevation of less than 1 mm [4,5]. Early repolarization pattern (ERP) is a relatively common variant of the normal ECG, which is observed in approximately 5% of the population [6]. This pattern is defined by J-point elevation of greater than or equal to 0.1 mV in greater than or equal to two inferior/lateral leads. When patients with ERP are resuscitated from otherwise unexplained syncope or polymorphic ventricular tachycardia and ventricular fibrillation (pVT/VF), the clinical condition is referred to as ERS [4]. In patients diagnosed as ERS, ERP in the lateral leads is referred to as ERS Type 1, in inferolateral leads is Type 2, and with a global pattern (inferolateral + anterior or right ventricular leads) is Type 3. Type 3 ERS is associated with the highest mortality rate, followed by Type 2; Type 1 had the lowest mortality rate [7].

The cellular mechanism underlying JWS has long been a matter of controversy. Two hypotheses have been advanced in the case of BrS: (i) the repolarization hypothesis proposed by Antzelevitch and co-workers. The repolarization hypothesis, is based on the observation that non-homogeneous repolarization in the different areas of right ventricular epicardium gives rise to phase 2 re-entry, leading to the development of closely coupled premature beats capable of inducing VT/VF [8,9]; (ii) the depolarization hypothesis proposed by Wilde and co-workers maintains that delayed conduction in the right ventricular outflow tract (RVOT) plays a principal role in the development of the arrhythmic and electrocardiographic manifestations due delayed conduction into the RVOT [10]. These hypotheses are not mutually exclusive and may be synergistic.

JWS has a clear familial predisposition, and mutations in the *CACNA1C* and *CACNB2b* genes have attracted recent attention [11–15]. Variants in the α_{1C}, β2b and $\alpha_2\delta$ subunits of the *L*-type calcium channel (LTCC) have previously been linked to a combined BrS and/or short QT phenotype. We present here a strong association of loss-of-function (LOF) mutations in the α_{1C} (*CACNA1C*) and β2b (*CACNB2b*) subunits with JWS. We use next-generation sequencing technology, cell transfection and whole-cell patch-clamp experiments to explore the potential relationship between calcium channel genetic variants and JWS, possible pathogenic mechanisms and possible approaches to therapy of patients carrying these variants.

2. Methods

(a) Analysis of clinical characteristics

Clinical and genetic studies were performed on 402 patients diagnosed with JWS and 420 healthy controls with no family history of arrhythmia, after approval of the ethics committee of the Renmin Hospital of Wuhan University and informed consent of the enrolled subjects. According to the most recent expert consensus statement, BrS is diagnosed when a value of greater than or equal to 3.5 is calculated using the Shanghai BrS scoring system. Diagnosis of ERS is made when a value of greater than or equal to 5.0 is obtained using the Shanghai ERS scoring system [16]. For each patient, we collected information on age at time of diagnosis, gender, clinical presentation, family history and therapy. P wave duration, PR interval, QT interval, QTc interval, QRS duration and Tp-e were measured from 12-lead ECGs. Patients with structural heart disease were excluded from the study.

(b) Genetic screening

Genomic DNA was extracted from peripheral blood leucocytes of patients according to standard protocols. Exons and exon–intron junction sequences of candidate genes were amplified by polymerase chain reaction (PCR). PCR products were purified with reagent (ExoSAPIT, USB, Cleveland, OH, USA) and the purified PCR products were sequenced in a loop on an ABI 3730 Genetic Analyzer (Applied Biosystem, Foster City, CA, USA). Sequencing results were confirmed by Mutation Surveyor v.4.0.8 software (Softgenetics, USA), and the above procedures were repeated for reconfirmation. According to the guidelines of the American College of Medical Genetics and Genomics (ACMG), the use of variant classifiers required variants to meet the criteria set out before they can be classified as pathogenic.

(c) Site-directed mutagenesis and transfection of cells

For the patch-clamp study, full-length human *CACNA1C* (wild-type, WT, or mutant) with enhanced yellow fluorescence protein (EYFP), *CACNB2b* (WT or mutant) cDNA, together with *CACNA2D1*-WT were cloned in the pcDNA3.1 vector (Invitrogen, Carlsbad, CA, USA) using site-directed mutagenesis. TSA201 cells were transfected with *CACNA1C*, *CACNB2b* and *CACNA2D1* plasmids used for electrophysiological studies [12,17]. cDNAs of the three LTCC subunits were co-transfected with a 1 : 1 : 1 molar ratio using Lipofectamine 2000 reagent (Invitrogen, Carlsbad, CA, USA). Electrophysiological studies were performed after 48–72 h of incubation.

(d) Cellular electrophysiology experiments

L-type calcium currents (I_{CaL}) were measured at room temperature (20–24°C) using an Axon-700B membrane clamp amplifier and PclampP10.4 software (Axon Instruments, San Francisco, CA, USA). Macroscopic whole-cell Ca^{2+} current was recorded by using bath solution perfusion containing (in mmol l^{-1}) 2 $CaCl_2$, 1 $MgCl_2$, 150 TEA, 10 HEPES and 10 glucose (PH 7.35 with CsOH). Patch pipettes were fabricated from borosilicate glass capillaries (1.5 mm O.D., Fisher Scientific, Pittsburgh, PA, USA), which were filled with the perfusion containing (in mmol l^{-1}) 110 CsCl, 0.1 $CaCl_2$, 10 HEPES, 10 EGTA, 2 MgATP and 10 TEA (PH7.35 with CsOH), with uncompensated access resistances of 1.0–2.8 MΩ. Recorded currents were filtered with an eight-pole Bessel filter at 5 kHz and digitized at 50 kHz. Series resistance was electronically compensated at 70–85%. Data were recorded and analysed with Pclamp v.10.4 (Axon Instruments, Sunnyvale, CA, USA), Excel (Microsoft, Redmond, WA, USA) and Origin 7.5 (Microcal Software, Northampton, MA, USA). The voltage-dependent steady-state activation (SSA) curve of I_{CaL} used a dual-pulse protocol in which the conditioned pulse was holding potential of −90 mV. The command potential was −50 to +60 mV in 10 mV step increments from the holding potential with 400 ms pulses. A Boltzmann function was fitted to the activation or inactivation curves with the pulse voltage as the horizontal axis and the whole-cell conductance as the vertical axis.

(e) Statistical analysis

Data were presented as mean ± s.d. unless otherwise noted. Comparisons between the two and multiple groups were performed with the Student's *t*-test or one-way ANOVA with Bonferroni correction, as appropriate. All data involving statistics were analysed using GraphPad software v.8.0. Differences were considered statistically significant at a value of $p < 0.05$.

3. Results

(a) Clinical characteristics of the probands and family members with mutations

We uncovered four probands carrying *CACNA1C*-G37R mutations and three carrying *CACNB2b*-S143F mutations. The clinical characteristics of JWS patients displaying calcium channel mutations are shown in table 1. The main symptoms at the time of diagnosis included syncope, SCD/VT/VF, premature ventricular contraction (PVC) and bradycardia.

Among all 402 JWS patients, the *CACNA1C*-G37R was identified in five cases from four families, two with a family history of SCD. Among the probands carrying the *CACNA1C*-G37R variant (four males, 100%; mean age 36.0 ± 11.0 years), two were diagnosed with BrS and two with ERS. One suffered from SCD/VF, PVC, bradycardia (25.0%) and two (50.0%) presented with syncope.

The *CACNB2b*-S143F mutation was uncovered in seven patients from three families, two with a family history of SCD. Among the probands carrying the *CACNB2b*-S143F variant, two presented with a phenotype of spontaneous Type 1 BrS and one with ERS (two males, 66.7%; mean age 52.3 ± 25.1 years). All three suffered from syncope (100.0%).

Compared with healthy controls, heart rate (HR) was strikingly slower in probands carrying *CACNB2b*-S143F; P wave duration was significantly longer in both mutant groups, and QTc interval was significantly shorter in *CACNA1C*-G37R carriers when compared with WT (table 2). Other variables, including HR in *CACNA1C*-G37R, QTc interval in *CACNB2b*-S143F and PR interval, QRS duration, Tp-e, and Tp-e/QT in both *CACNA1C*-G37R and *CACNB2b*-S143F, did not differ significantly between control and the two mutation groups (table 2). Table 3 shows the ECG parameters of JWS patients carrying the calcium channel mutations. HR, P wave duration and QTc interval but not Tp-e were significantly different between *CACNA1C*-G37R carriers and healthy controls.

The younger brother of proband 1, who carried *CACNA1C*-G37R, had ERS and died at age of 25 suddenly during vagal circumstances (figure 1*a*). At 23 years of age, his ECG showed typical Type 3 ERP and bradycardia. Because of his positive family history and genetic results, quinidine was administrated. Quinidine led to a dramatic increase of QTc from 343.5 to 447.8 ms, and a significant decrease of the J wave in inferior and lateral leads (figure 1*e*). Proband 2, a 31-year-old man (figure 1*b*) presented with an ECG displaying ERP in anterior leads as well as multiple PVC (figure 1*f*). His deceased brother had the same pattern on his ECG and his father died of SCD at age 50 years. Type 1 Brugada ECG was observed after ajmaline provocation in probands 3 and 4 (figure 1*c*,*d*). Both presented with syncope but had a negative family history. Their ECGs both showed significant elevation of a coved-type ST-segment (greater than or equal to 0.2 mm) in the right precordial leads V1–V2.

Among *CACNB2b*-S143F carriers, probands 5 and 7 both exhibited spontaneous Type 1 ECG patterns in the right precordial leads (figure 2*d*,*f*), whereas proband 6 presented with an ERS phenotype and a history of syncope (figure 2*e*). As shown in figure 2, QTc interval was shorter than normal in probands 5 and 6 (QTc = 375 and 365 ms). Proband 7 had normal QT (QTc = 439 ms), likely due to additional genetic variants (see below).

Table 1. Clinical characteristics of J wave syndrome probands carrying calcium channel mutations.

index	*CACNA1C*-G37R (*n* = 4)	*CACNB2b*-S143F (*n* = 3)
age (years)	36.0 ± 11.0	52.3 ± 25.1
male, *n* (%)	4 (100.0)	2 (66.7)
symptom, n (%)		
syncope	2 (50.0)	3 (100.0)
SCD/VT/VF	1 (25.0)	0
PVC	1 (25.0)	0
bradycardia	1 (25.0)	0
asymptomatic	1 (25.0)	0
family history of SCD	2 (50.0)	2 (66.7)

(b) Genetic discovery of calcium mutations in J wave syndrome

Genetic analysis revealed two heterozygous missense mutations in the α_{1C} (*CACNA1C*) and β2b (*CACNB2b*) subunits of LTCC in seven probands (figure 3), five (71.4%) of which harboured additional genetic variants, such as *CACNB2B*-D601E, *SCN1B*-L210P, *SCN5A*-H558R, *KCNH2*-K897T, *KCNE1*-G38S, *KCNH2*-R1047L. These calcium channel variants were not present in 450 reference control alleles. The *CACNA1C* gene was mutated from a G to A substitution at location 109 in exon 2, resulting in an amino acid change from glycine to arginine at position 37 (G37R, figure 3*a*). The *CACNB2b* gene was mutated with substitution of T for C at position 428 in exon 5, resulting in an amino acid change from serine to phenylalanine at position 143 (S143F, figure 3*b*). Additionally, we evaluated the pathogenicity of both missense substitutions using multiple prediction tools, including Mutation Taster, PolyPhen-2, SIFT, REVEL, MetaLR and ClinVar (table 4). The majority of prediction tools predicted 'disease causing' or 'damaging' variants with a global minor allele frequency (MAF) < 0.001 for each in the 1000 Genomes database.

(c) Functional expression of *CACNA1C*-G37R and *CACNB2b*-S143F

Expression studies using whole-cell patch-clamp techniques to evaluate the effect of *CACNA1C*-G37R and *CACNB2b*-S143F mutations were performed. Representative I_{CaL} tracings of voltage-dependent activation are shown in figures 4*a* and 5*a*. From a holding potential of −90 mV voltage was depolarized to various potentials until +10 mV (figures 4*b* and 5*b*). Current–voltage relationships (*I*–*V* curves) showed that homozygous expression of *CACNA1C*-G37R reduced I_{CaL} by 90.3% (25.4 ± 4.4 pA/pF versus 2.5 ± 1.7, $n = 12, 13$; $^*p < 0.05$), and by 72.7% in the case of heterozygous expression (25.4 ± 4.4 pA/pF versus 6.9 ± 3.0, $n = 12, 12$; $^*p < 0.05$) when compared to WT (figure 4*c*). Homozygous expression of *CACNB2b*-S143F reduced I_{CaL} by 80.7% (25.4 ± 4.4 pA/pF versus 4.9 ± 3.4 pA/

Table 2. ECG parameters in J wave syndrome probands carrying calcium channel gene mutations. If $p < 0.05$, it is shown in italics (mean ± s.d.). *p*-value indicates the statistical difference between study group versus healthy controls.

index	healthy control ($n = 420$)	*CACNA1C*-G37R ($n = 4$)	*p*-value	*CACNB2b*-S143F ($n = 3$)	*p*-value
HR (bpm)	72.7 ± 8.9	69.0 ± 11.7	0.410	62.5 ± 11.4	*0.049*
P wave duration (ms)	87.6 ± 9.1	99.0 ± 22.9	*0.015*	113.3 ± 5.8	*<0.001*
PR interval (ms)	170.7 ± 18.7	175.0 ± 19.1	0.647	178.7 ± 35.9	0.464
QRS duration (ms)	89.4 ± 14.6	100.5 ± 17.2	0.131	98.0 ± 13.1	0.310
QTc interval (ms)	408.2 ± 21.4	377.0 ± 23.4	*0.004*	393.2 ± 40.1	0.230
Tp-e	82.3 ± 9.9	90.0 ± 8.2	0.122	80.0 ± 0.0	0.643
Tp-e/QT	0.22 ± 0.05	0.25 ± 0.02	0.232	0.20 ± 0.01	0.489

Table 3. ECG parameters of J wave syndrome patients carrying calcium channel gene mutations. If $p < 0.05$, it is shown in italics (mean ± s.d.). *p*-value indicates the statistical difference between study group versus healthy controls.

index	healthy control ($n = 420$)	*CACNA1C*-G37R ($n = 5$)	*p*-value	*CACNB2b*-S143F ($n = 7$)	*p*-value
HR (bpm)	72.7 ± 8.9	69.8 ± 10.2	0.470	65.8 ± 10.9	*0.043*
P wave duration (ms)	87.6 ± 9.1	103.2 ± 21.9	*<0.001*	108.0 ± 16.4	*<0.001*
PR interval (ms)	170.7 ± 18.7	176.0 ± 16.7	0.529	165.2 ± 33.2	0.448
QRS duration (ms)	89.4 ± 14.6	98.4 ± 15.6	0.172	92.8 ± 12.2	0.541
QTc interval (ms)	408.2 ± 21.4	378.7 ± 20.6	*0.002*	396.6 ± 29.0	0.158
Tp-e	82.3 ± 9.9	92.0 ± 8.4	*0.030*	82.0 ± 11.0	0.937
Tp-e/QT	0.22 ± 0.05	0.26 ± 0.02	0.075	0.22 ± 0.02	1.000

pF, $n = 12, 8$; $^*p < 0.05$), and by 51.0% in the case of heterozygous expression (25.4 ± 4.4 pA/pF versus 12.5 ± 4.5 pA/pF, $n = 12, 9$; $^*p < 0.05$) at 0 mV when compared to WT (figure 5*c*).

The half-activation voltage ($V_{1/2}$) was obtained by fitting the activation conductance variables (I/I_{max}), and there was no significant difference observed between *CACNA1C*-WT and *CACNA1C*-G37R groups (*CACNA1C*-WT versus *CACNA1C*-G37R: −11.91 ± 0.45 mV versus −14.51 ± 1.43 mV, $n = 12, 13$; $p > 0.05$; figure 4*d*). Similarly, no significant difference in steady-state inactivation was found between the two groups (*CACNA1C*-WT versus *CACNA1C*-G37R: −30.90 ± 1.45 mV versus −32.65 ± 1.87 mV, $n = 12, 6$; $p > 0.05$; figure 4*e*). However, there was a significant acceleration in steady-state activation and inactivation for *CACNB2b*-S143F compared with *CACNB2b*-WT (*CACNB2b*-WT versus *CACNB2b*-S143F: −11.91 ± 0.45 mV versus −18.02 ± 1.47 mV, $n = 12, 8$ for activation, $p < 0.01$; *CACNB2b*-WT versus *CACNB2b*-S143F: −30.90 ± 1.45 mV versus −39.83 ± 1.74 mV, $n = 12, 6$ for inactivation, $p < 0.01$, respectively; figure 5*d*,*e*). The results showed a significant negative shift in steady-state activation and even larger negative shifts in steady-state inactivation when the mutant β2b-subunit were expressed. In summary, the results of the patch clamp experiments revealed significant LOF in the cardiac calcium channel activity of both *CACNA1C*-G37R and *CACNB2b*-S143F mutations.

4. Discussion

Age and gender of our JWS probands carrying *CACNA1C*-G37R, are similar to that reported previously, 74.1–92.0% of JWS patients were male, with a mean age at time of onset of 30–42 years [16,18,19]. These classic features were not observed in the JWS probands carrying *CACNB2b*-S143F. Average age at time of onset was much older (52.3 ± 25.1) and male predominance was lower (66.7%). This may not be representative due to the small sample size, selection bias or due to factors such as female gender or genetic variants that predispose to long QT syndrome [12]. BrS patients are known to develop symptoms between 20 and 65 years of age. ERS tends to occur in younger people, especially in men, possibly due to high levels of testosterone, and higher vagal tone [16]. In recent work from our group, ERS probands were 7.5 years younger than BrS probands [20]. In the present study, we observed a similar disparity among BrS and ERS probands with same mutation (*CACNA1C*-G37R or *CACNB2b*-S143F). The difference likely depends on the distinctions between the electrophysiological mechanisms underlying BrS and ERS.

Most arrhythmic events and SCD typically occur during episodes of vagal predominance and/or bradycardia which is normally associated with the appearance of accentuated J waves and ST-segment elevation [16,21,22]. Notably, the younger brother of proband 1 died suddenly during episodes of vagal predominance. This is consistent with the results of Viskin *et al*. who proposed that both a history of syncope at rest and bradycardia have a strong association with risk in cases of ERS, contributing to pause-dependent augmentation of ST-segment elevation leading to VF [23]. These findings support the notion that changes in vagal tone increase arrhythmic risk. It is for this reason that, sympathetic mimic drug is an option in the approach to therapy.

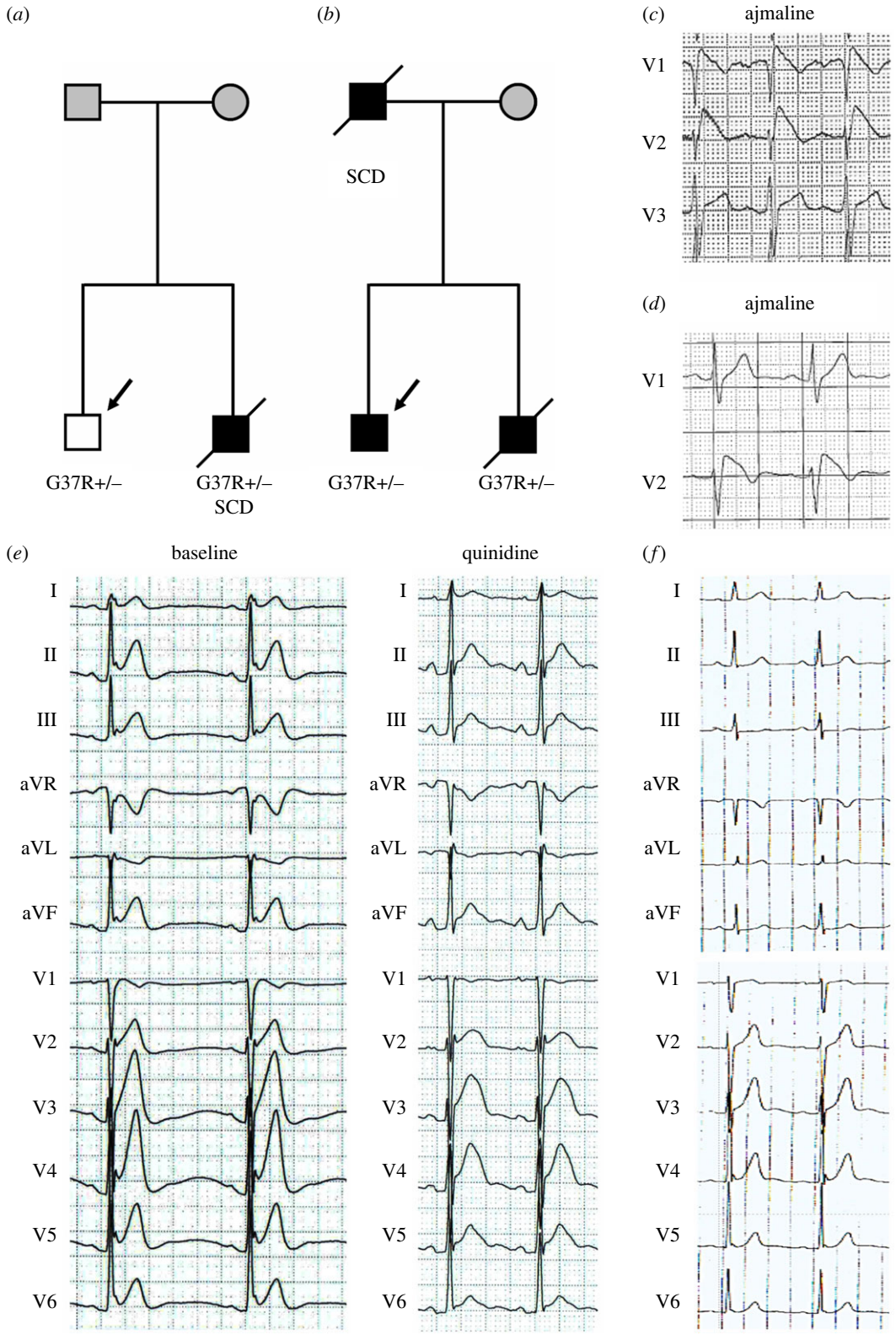

Figure 1. Pedigrees of representative families and ECGs of JWS patients carrying *CACNA1C*-G37R. (*a*) The family members included proband 1 and his deceased younger brother with a history of SCD. (*b*) Proband 2 and his deceased younger brother both presented with ERS/SQT, and the father died of SCD at age of 50 years. (*c*) The ECG of proband 3 shows an ajmaline-induced Type 1 pattern in leads V1 and V2. (*d*) After ajmaline provocation, ECG of proband 4 is characterized by a coved ST-segment elevation in leads V1 and V2. (*e*) ECG of proband 1 is presented at baseline and after treatment with quinidine. He shows significant decrease of ST-segment in leads V2–V6 and remained asymptomatic on quinidine. (*f*) ECG of proband 2 showing spontaneous ERP in anterior leads. Squares indicate male subjects, circles female subjects and symbols with a slash mark deceased individuals. The arrows indicate the probands and pointed triangle indicates twins. −/− wild-type (WT); +/− heterozygous for the mutation. The symptomatic subjects are labelled by black. The asymptomatic subjects are shown as white and unaffected subjects are labelled by dark grey. (Online version in colour.)

Family history of SCD is an important risk factor in clinical practice. JWS is related to vulnerability for the development of SCD, pVT and VF in patients with structurally normal hearts [24,25]. A meta-analysis by Rattanawong *et al.* [26] found that a family history of SCD in BrS patients less than 40 years of age doubled the risk of a major

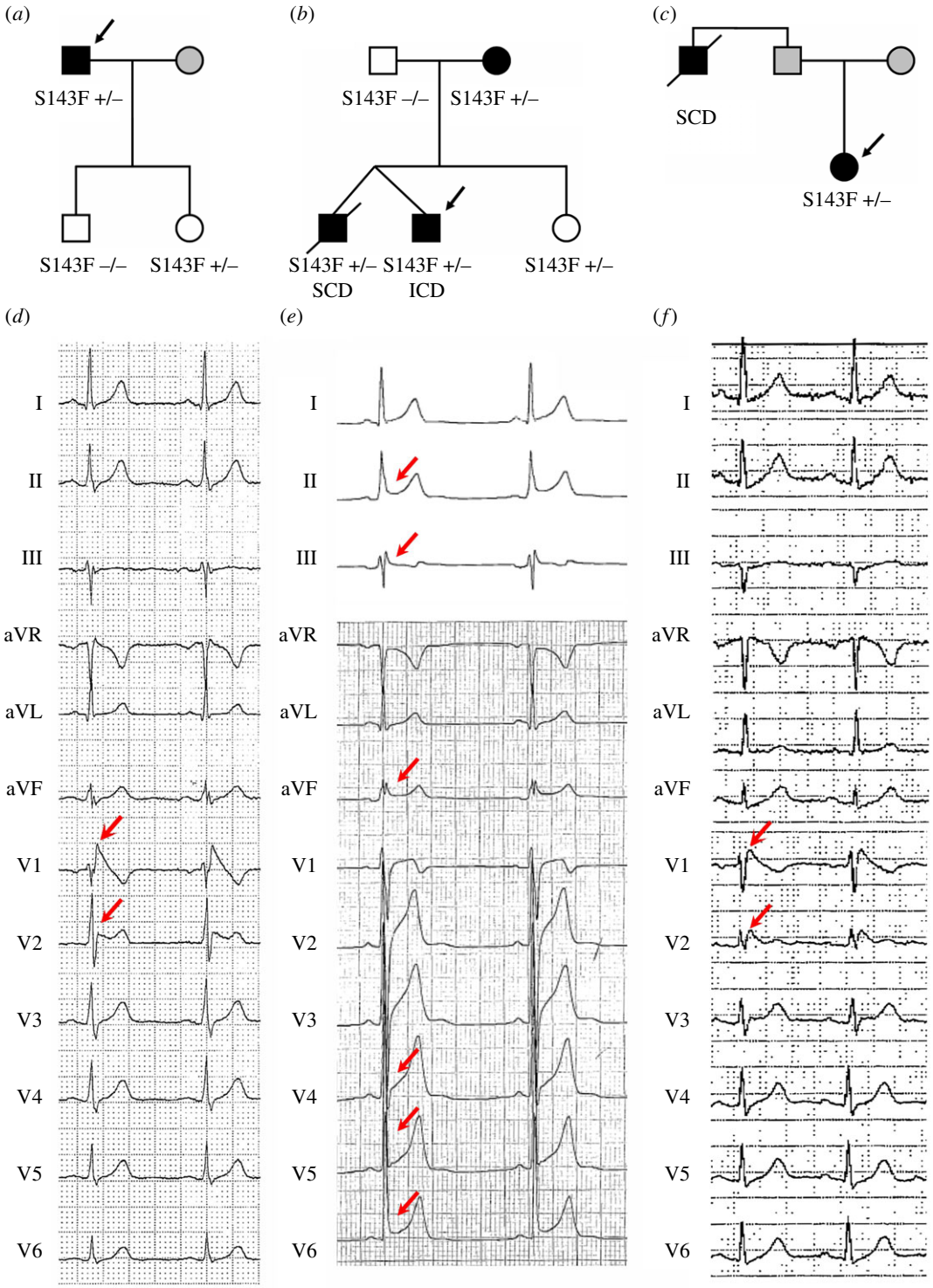

Figure 2. Pedigrees of representative families and ECGs of JWS patients carrying *CACNB2b*-S143F. (*a*) Family members with a BrS phenotype include a father and his daughter; the genetic result of his son is negative. (*b*) Proband 6, his mother and his twin brother present mutation-positive with a ERS phenotype, whereas his sister is a silent carrier. He eventually received implantable cardioverter–defibrillator (ICD) therapy. (*c*) Proband 7 exhibits a BrS phenotype; his father died of SCD. (*d*) The ECG of proband 5 shows a spontaneous Type 1 ECG pattern in lead V1–V2. (*e*) ECG of proband 6 is characterized by J-point elevation greater than or equal to 1 mm in contiguous inferior and lateral leads. (*f*) ECG of proband 7 shows significant ST-segment elevation (Type 1) in leads V1–V2. (Online version in colour.)

arrhythmic event (MAE). Previous reports also suggested the family history of SCD in ERS ranges from 13% to 18% [27,28]. Interestingly, Hu *et al*. recently reported that approximately 34% of *SCN5A*$^{+}$ JWS probands have a family history of unexplained SCD, suggesting a worse outcome in this scenario [20]. Our results show that 50.0% of *CACNA1C*-G37R and 66.7% of *CACNB2b*-S143F have a family history of SCD among JWS probands. These findings call for close follow-up of survivors who have a family history of unexplained SCD at a young age.

We assume that carriers of calcium mutations with LOF will have a shorter QTc interval. A report by Antzelevitch *et al*. [13], is the first to associate LTCC mutations with a combined BrS phenotype and shorter than normal QT interval. Napolitano and co-workers confirmed that *CACNA1C* is an infrequent but definitive cause of BrS, typically associated

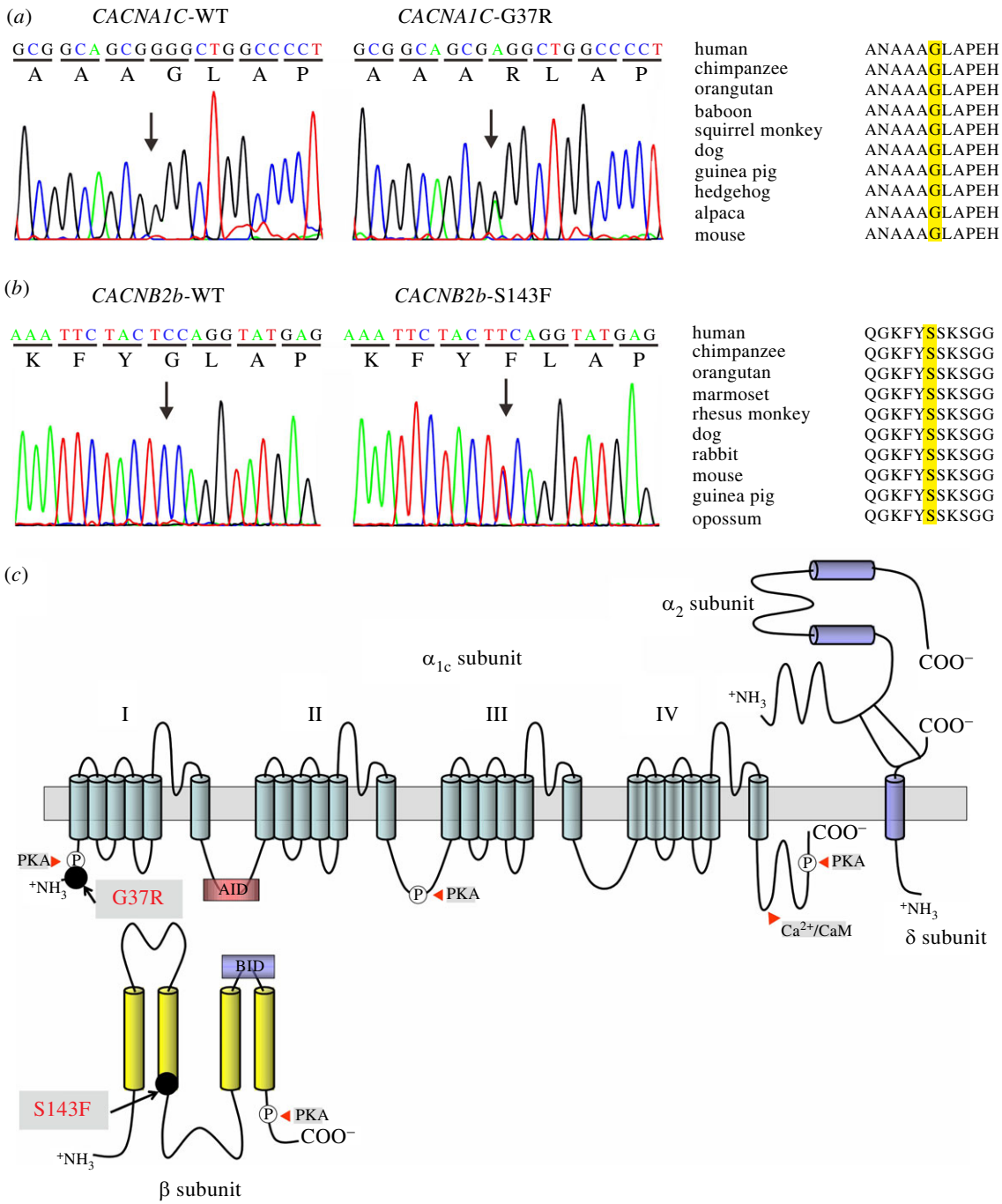

Figure 3. Genetic analysis of *CACNA1C*-G37R and *CACNB2b*-S143F. (*a*) Electropherogram of *CACNA1C*-WT and *CACNA1C*-G37R and amino acid sequence alignment of *CACNA1C*-G37R. (*b*) Electropherogram of *CACNB2b*-WT and *CACNB2b*-S143F and amino acid sequence alignment of *CACNB2b*-S143F. (*c*) Schematic of the $Ca_V1.2$ channel pore-forming α_{1C} subunit and the auxiliary $\alpha_2\delta$ and β subunits. The *CACNA1C*-G37R mutation is in the *N*-terminus close to the PKA binding site (black circle). The *CACNB2b*-S143F mutation is located at the Hook region. Phosphorylation sites by PKA and calcineurin (CaN) binding sites located in $Ca_V1.2$ and β subunits (white cycles with P). BID, β subunit interacting domain and AID, α subunit interacting domain. (Online version in colour.)

with a short QTc interval (371 ms) [11]. Our team identified a short QTc interval not only in ERS with single calcium channel mutation (387 ms), but also in a hypertrophic cardiomyopathy patient carrying a calcium channel mutation [14,29]. Here, we observed that QT/QTc intervals are typically shorter than normal in JWS probands carrying *CACNA1C*-G37R when compared with healthy controls, but QT/QTc intervals are normal in JWS probands carrying *CACNB2b*-S143F. We believe that this is due to the complex genetic background in our *CACNB2b*-S143F probands. For example, proband 7 has a normal QTc interval most likely resulting from additional genetic variants (*CACNB2b*-D601E, *KCNH2*-R1047L and K897T), which are known to prolong QTc interval by augmenting I_{CaL} or reducing I_{Kr} [17,30]. The opposing influence of these additional gene variants can account for the appearance of a longer QT interval in JWS patients [17].

The ST–T wave morphology changes in JWS are thought to be attributable to genetically mediated alterations in the interplay between depolarizing or repolarizing cardiac currents, which includes genes regulating the sodium current (I_{Na}), the *L*-type calcium current (I_{CaL}) or the transient outward potassium current (I_{to}) [31]. Specifically, an increase in I_{Na} contributes to a reduction in the depolarization of the cardiac action potential (AP), while I_{CaL} is responsible for the plateau phase of the cardiac AP, both of which can promote

Table 4. Summary of J wave syndrome probands carrying calcium channel gene mutations G37R and S143F.

	CACNA1C-G37R	*CACNB2b*-S143F
reported ID	rs34534613	rs150528041
variant type	missense	missense
nucleotide change	c.109G > A	c.428C > T
exon location	2	5
MAF		
GnomAD	0.003464	0.000510
ExAC	0.007385	0.000509
1000 Genomes	0.000399	0.000399
SIFT		
score	0.000	0.010
prediction	deleterious	deleterious
PolyPhen-2		
score	0.967	0.730
prediction	probably damaging	possibly damaging
Mutation Taster		
score	1	1
prediction	disease causing	disease causing
MetaLR		
score	0.903	0.703
prediction	damaging	damaging
REVEL		
score	0.655	0.611
prediction	likely disease causing	likely disease causing
ClinVar		
score	two stars	a star
prediction	benign/likely benign	uncertain significance/ likely benign

early repolarization. Additionally, Ito contributes to the phase 1 of AP. At the ion channel level, a reduction of inward currents (I_{Na} or I_{CaL}) or increase in outward delayed rectifier potassium currents (I_{Kr} or $I_{K\text{-}ATP}$) gives the I_{to} the possibility to accentuate phase 1 repolarization. I_{to} is a prominent repolarizing current that partially repolarizes the membrane in physiological conditions, determining the rapid repolarization of the AP and setting the amplitude of the plateau, which gives rise to the spike-and-dome AP morphology and presents as prominent J wave in ECG [32].

Quinidine is the only currently recognized antiarrhythmic drug with inhibition on the outward potassium currents (I_{to}, I_{Kr}, etc.), which can effectively prevent spontaneous or induced VF in JWS [28,33]. The responsiveness to quinidine by BrS carrying calcium channel mutations was first reported by Antzelevitch *et al*. [13]. We provide additional evidence for the responsiveness of JWS patients to quinidine. The ability of quinidine to prevent induction of VT/VF and its effect to prolong QTc interval in proband 1 is consistent with earlier reports [5,33,34]. Unfortunately, the use of quinidine is currently limited due to a lack of drug availability [35]. Furthermore, electrical storms can be suppressed with β-adrenergic agents, such as isoproterenol capable of augmenting the LTCC [36]. Additional pharmacological therapy includes cilostazol and milrinone, a phosphodiesterase III inhibitor, which have a significant role in the improvement of JWS by augmenting I_{CaL} as well as reducing I_{to} [37,38]. However, large clinical studies are still needed to further demonstrate their safety and benefit to patients with JWS. Recently, a new discovery from Antzelevitch and Ackerman showing that acacetin, a natural flavonoid, has a potent blocking effect on I_{to} in canine ventricular myocytes as well as human iPS-derived cardiomyocytes and capable of preventing the development of pVT in experimental wedge and whole-heart models of BrS and ERS, including models induced by calcium blocker [8,39,40]. In fact, we first observe quinidine is highly effective in our ERS case carried *CACNA1C*-G37R mutation. However, the full extent of quinidine's effect on the properties of calcium channels in patients with mutations is not yet fully understood and warrants further investigation. It should be noted that further experiments of transgenic models are needed to confirm this mechanism.

Variants in genes encoding the calcium channels including *CACNA1C* (Cav1.2), *CACNB2b* (Cavβ2b) and *CACNA2D1* (Cav$\alpha_2\delta$) have been reported in up to 13% of probands [12,13,41]. Antzelevitch and co-workers first identified nine mutations of the *CACNA1C* gene in patients diagnosed with BrS, ERS and idiopathic VF, including A39V, G490R, V2014I, E1829-Q1833dup, E850del, R1880Q, D2130N, E1115K and C1837Y, of which the first four cause functional deletion of I_{Ca} [12,13]. Subsequently, Napolitano *et al*., identified nine additional potentially pathogenic mutations in *CACNA1C* including Q428E, A1648T, T320M, E850D, N1255S, A1717G, R1880Q, E850del, and G2084E. It is noteworthy that Fukuyama *et al*. study pathogenic mutations of LTCC-related genes in 312 probands with a diagnosis of BrS, ERS and short QT syndrome, consequently discovering six gene mutations: *CACNA1C*, N547S, R632R, R858H, R1780H, C1855Y and R1910Q [42]. Among them, five were potentially pathogenic *CACNA1C* mutations reported twice, including T320M, A1648T, A1717G, R1880Q and E850del. We sequenced 402 JWS patients and their families and identified four JWS probands carrying *CACNA1C*-G37R mutation and three carrying *CACNB2b*-S143F mutation. Functional evidence of those two mutation groups both show significant reduction of I_{CaL} density. Their kinetics were also significantly accelerated, displaying a LOF of I_{CaL} in both. Our results support the conclusion that *CACNA1C*-G37R and *CACNB2b*-S143F are two hotspots among the rare mutations in the cardiac calcium channels associated with a JWS phenotype.

(a) Study limitations

The small number of affected individuals in our study is susceptible to selection, and referral biases. Secondly, this work lacks long-term follow-up with these patients, especially those with a high risk of malignant arrhythmias. Finally, our functional study would be ideal if detailed assessment of other variants contributing to the complex genetic background were presented.

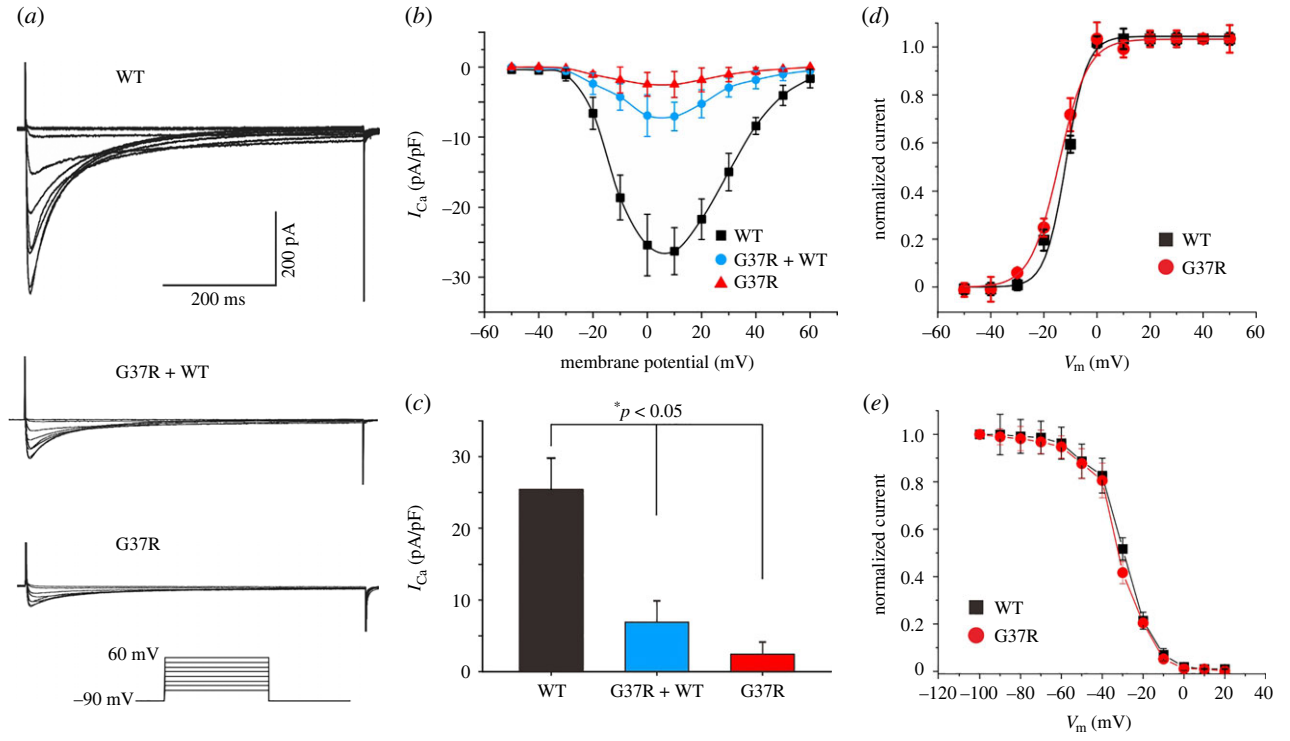

Figure 4. Functional expression of *CACNA1C*-G37R on I_{CaL}. (*a*) Representative I_{CaL} recordings from TSA201 cells expressing *CACNA1C*-WT, *CACNA1C*-G37R + WT and *CACNA1C*-G37R ($n = 12, 12, 13$, respectively). (*b*) Current density–voltage relationships for *CACNA1C*-WT, *CACNA1C*-G37R + WT and *CACNA1C*-G37R. (*c*) Bar graph depicting peak I_{CaL} density at 0 mV for *CACNA1C*-WT, *CACNA1C*-G37R + WT and *CACNA1C*-G37R channels. Data are expressed as mean + s.e.m. (*$p < 0.05$, compared with *CACNA1C*-G37R + WT. *$p < 0.05$, compared with *CACNA1C*-G37R). (*d*) Steady-state activation curve of I_{CaL} for *CACNA1C*-WT and *CACNA1C*-G37R. (*e*) Steady-state inactivation curve of I_{CaL} for *CACNA1C*-WT and *CACNA1C*-G37R. (Online version in colour.)

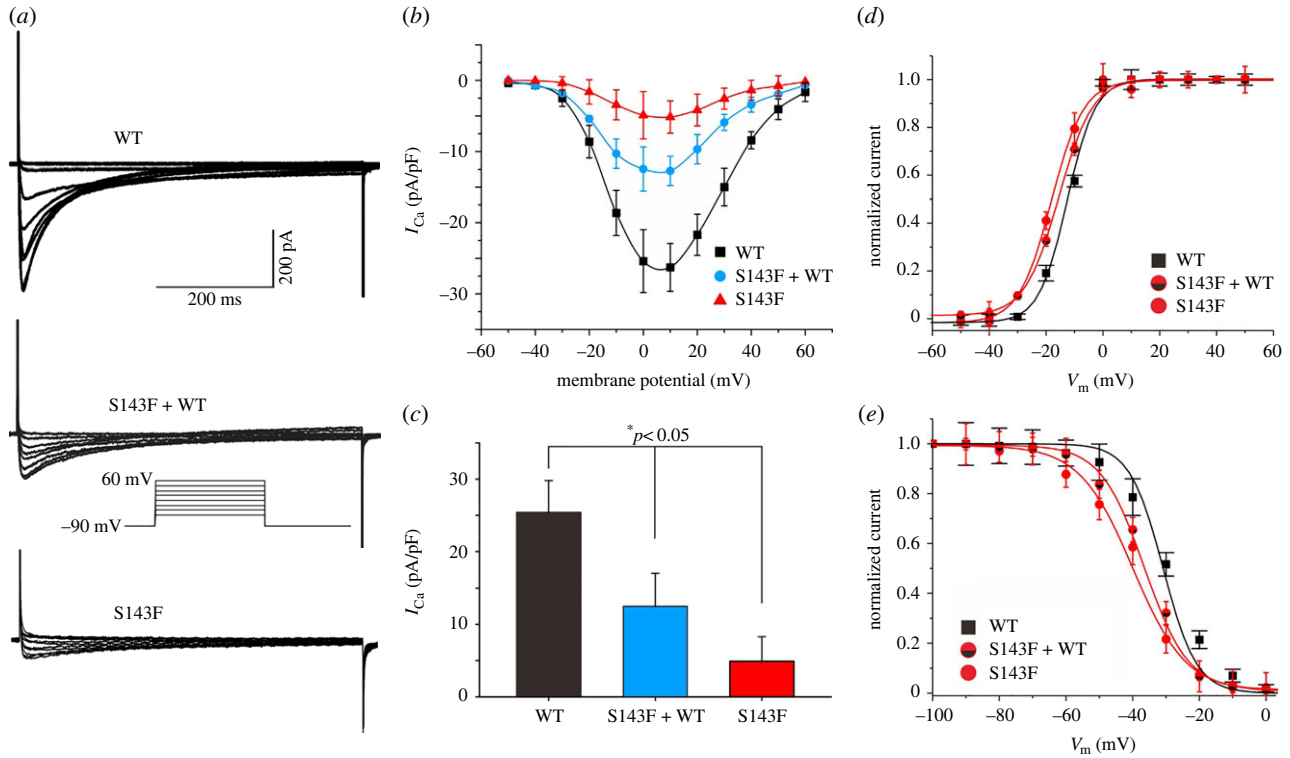

Figure 5. Functional expression of *CACNB2b*-S143F on I_{CaL}. (*a*) Representative I_{CaL} recordings from TSA201 cells expressing *CACNB2b*-WT, *CACNB2b*-S143F + WT and *CACNB2b*-S143F ($n = 12, 9, 8$, respectively). (*b*) Current density–voltage relationships for *CACNB2b*-WT, *CACNB2b*-S143F + WT and *CACNB2b*-S143F. (*c*) Bar graph depicting peak I_{CaL} density at 0 mV for *CACNB2b*-WT, *CACNB2b*-S143F + WT and *CACNB2b*-S143F channels. Data are expressed as mean + s.e.m. (*$p < 0.05$, compared with *CACNA1C*-S143F + WT. *$p < 0.05$, compared with *CACNA1C*-S143F). (*d*) Steady-state activation curve of I_{CaL} for *CACNB2b*-WT and *CACNB2b*-S143F. (*e*) Steady-state inactivation curve of I_{CaL} for *CACNB2b*-WT and *CACNB2b*-S143F. (Online version in colour.)

5. Conclusion

Genetic and functional studies identify two high-frequency LOF mutations, including *CACNA1C*-G37R and *CACNB2b*-S143F, which are definitive causes of JWS with a family history of SCD. We also provide additional evidence for the effectiveness of quinidine in this setting. JWS patients carrying these two common pathogenic mutations are clinically characterized by prolonged P wave duration. However, there are some clinical differences between *CACNA1C*-G37R and *CACNB2b*-S143F mutations. The former is associated with significantly shorter QTc intervals, while the latter is linked to a significant slowing of HR.

Ethics. This study is approved by the ethics committee of the Renmin Hospital of Wuhan University.

Data accessibility. All datasets generated for this study are available from the corresponding author upon reasonable request.

Authors' contributions. B.Z.: conceptualization, data curation, formal analysis, investigation, methodology, software, visualization, writing—original draft, writing—review and editing; X.Z.: conceptualization, data curation, investigation, methodology, visualization, writing—original draft, writing—review and editing; R.S.: data curation, investigation, resources, writing—review and editing; A.P.: data curation, funding acquisition, resources, writing—review and editing; M.G.: formal analysis, methodology, resources, writing—review and editing; C.A.: conceptualization, funding acquisition, project administration, resources, validation, writing—review and editing; D.H.: conceptualization, formal analysis, funding acquisition, methodology, project administration, software, supervision, validation, visualization, writing—original draft, writing—review and editing; H.B.-M.: conceptualization, data curation, formal analysis, funding acquisition, project administration, resources, supervision, validation, writing—original draft, writing—review and editing.

All authors gave final approval for publication and agreed to be held accountable for the work performed therein.

Conflict of interest declaration. C.A. served as a consultant and received grant funds from Novartis and Trevena Inc. All other authors report no relationships to disclose.

Funding. This work was supported by the National Natural Science Foundation Project of China (grant nos. 82270332 and 81670304, to D.H.), the Fundamental Research Funds for the Central Universities of China (grant no. 2042022kf1217 to D.H.), the National Institutes of Health of USA (NIH R56 (HL47678), NIH R01 (HL138103), NIH R01 (HL152201) to C.A. and H.B.-M.), the W.W. Smith Charitable Trust and the Wistar and Martha Morris Fund to C.A., the W.W. Smith Charitable Trust and Sharpe-Strumia Research Foundation to H.B.-M.

Acknowledgements. We are grateful to Dr Michel Springer, a cardiology specialist in Louisville, KY, USA, for providing clinical information; Dr Sami Viskin, from Department of Cardiology, Tel Aviv Sourasky Medical Center and Sackler School of Medicine, Tel Aviv University, Israel, for providing clinical information and Ryan Pfeiffer from the Masonic Medical Research Institute, USA, for technical assistance.

References

1. Antzelevitch C, Yan GX. 2010 J wave syndromes. *Heart Rhythm.* **7**, 549–558. (doi:10.1016/j.hrthm.2009.12.006)
2. European Heart Rhythm A. 2006 ACC/AHA/ESC 2006 guidelines for management of patients with ventricular arrhythmias and the prevention of sudden cardiac death: a report of the American College of Cardiology/American Heart Association Task Force and the European Society of Cardiology Committee for Practice Guidelines (Writing Committee to Develop Guidelines for Management of Patients With Ventricular Arrhythmias and the Prevention of Sudden Cardiac Death). *J. Am. Coll. Cardiol.* **48**, e247–e346. (doi:10.1016/j.jacc.2006.07.010)
3. Fishman GI *et al.* 2010 Sudden cardiac death prediction and prevention: report from a National Heart, Lung, and Blood Institute and Heart Rhythm Society Workshop. *Circulation* **122**, 2335–2348. (doi:10.1161/CIRCULATIONAHA.110.976092)
4. Antzelevitch C *et al.* 2005 Brugada syndrome: report of the second consensus conference: endorsed by the Heart Rhythm Society and the European Heart Rhythm Association. *Circulation* **111**, 659–670. (doi:10.1161/01.CIR.0000152479.54298.51)
5. Priori SG *et al.* 2015 ESC Guidelines for the management of patients with ventricular arrhythmias and the prevention of sudden cardiac death: the Task Force for the Management of Patients with Ventricular Arrhythmias and the Prevention of Sudden Cardiac Death of the European Society of Cardiology (ESC). Endorsed by: Association for European Paediatric and Congenital Cardiology (AEPC). *Eur. Heart J.* **36**, 2793–2867. (doi:10.1093/eurheartj/ehv316)
6. Antzelevitch C *et al.* 2017 J-wave syndromes expert consensus conference report: emerging concepts and gaps in knowledge. *Europace* **19**, 665–694.
7. Priori SG *et al.* 2013 HRS/EHRA/APHRS expert consensus statement on the diagnosis and management of patients with inherited primary arrhythmia syndromes: document endorsed by HRS, EHRA, and APHRS in May 2013 and by ACCF, AHA, PACES, and AEPC in June 2013. *Heart Rhythm.* **10**, 1932–1963. (doi:10.1016/j.hrthm.2013.05.014)
8. Di Diego JMA *et al.* 2020 Acacetin suppresses the electrocardiographic and arrhythmic manifestations of the J wave syndromes. *PLoS ONE* **15**, e0242747. (doi:10.1371/journal.pone.0242747)
9. Schwartz PJ *et al.* 2020 Inherited cardiac arrhythmias. *Nat. Rev. Dis. Primers* **6**, 58. (doi:10.1038/s41572-020-0188-7)
10. Morita H, Zipes DP, Wu J. 2009 Brugada syndrome: insights of ST elevation, arrhythmogenicity, and risk stratification from experimental observations. *Heart Rhythm.* **6**, S34–S43. (doi:10.1016/j.hrthm.2009.07.018)
11. Novelli V *et al.* 2022 Role of CACNA1C in Brugada syndrome: prevalence and phenotype of probands referred for genetic testing. *Heart Rhythm.* **19**, 798–806. (doi:10.1016/j.hrthm.2021.12.032)
12. Burashnikov E *et al.* 2010 Mutations in the cardiac L-type calcium channel associated with inherited J-wave syndromes and sudden cardiac death. *Heart Rhythm.* **7**, 1872–1882. (doi:10.1016/j.hrthm.2010.08.026)
13. Antzelevitch C *et al.* 2007 Loss-of-function mutations in the cardiac calcium channel underlie a new clinical entity characterized by ST-segment elevation, short QT intervals, and sudden cardiac death. *Circulation* **115**, 442–449. (doi:10.1161/CIRCULATIONAHA.106.668392)
14. Chen X *et al.* 2021 Clinical and functional genetic characterization of the role of cardiac calcium channel variants in the early repolarization syndrome. *Front. Cardiovasc. Med.* **8**, 680819. (doi:10.3389/fcvm.2021.680819)
15. Sutphin BS *et al.* 2016 Molecular and functional characterization of rare CACNA1C variants in sudden unexplained death in the young. *Congenit. Heart Dis.* **11**, 683–692. (doi:10.1111/chd.12371)
16. Antzelevitch C *et al.* 2016 J-wave syndromes expert consensus conference report: emerging concepts and gaps in knowledge. *Heart Rhythm.* **13**, e295–e324. (doi:10.1016/j.hrthm.2016.05.024)
17. Hu D *et al.* 2010 Dual variation in SCN5A and CACNB2b underlies the development of cardiac conduction disease without Brugada syndrome. *Pacing Clin. Electrophysiol.* **33**, 274–285. (doi:10.1111/j.1540-8159.2009.02642.x)
18. Voskoboinik A *et al.* 2020 The many faces of early repolarization syndrome: a single-center case series. *Heart Rhythm.* **17**, 273–281. (doi:10.1016/j.hrthm.2019.09.013)
19. Kamakura T *et al.* 2020 Long-term prognosis of patients with J-wave syndrome. *Heart* **106**, 299–306. (doi:10.1136/heartjnl-2019-315007)
20. Zhang ZH *et al.* 2021 Distinct features of probands with early repolarization and Brugada syndromes carrying SCN5A pathogenic variants. *J. Am. Coll.*

Cardiol. **78**, 1603–1617. (doi:10.1016/j.jacc.2021.08.024)

21. Aizawa Y *et al.* 2012 Dynamicity of the J-wave in idiopathic ventricular fibrillation with a special reference to pause-dependent augmentation of the J-wave. *J. Am. Coll. Cardiol.* **59**, 1948–1953. (doi:10.1016/j.jacc.2012.02.028)
22. Kalla H, Yan GX, Marinchak R. 2000 Ventricular fibrillation in a patient with prominent J (Osborn) waves and ST segment elevation in the inferior electrocardiographic leads: a Brugada syndrome variant? *J. Cardiovasc. Electrophysiol.* **11**, 95–98. (doi:10.1111/j.1540-8167.2000.tb00743.x)
23. Rosso R *et al.* 2008 J-point elevation in survivors of primary ventricular fibrillation and matched control subjects: incidence and clinical significance. *J. Am. Coll. Cardiol.* **52**, 1231–1238. (doi:10.1016/j.jacc.2008.07.010)
24. Haissaguerre M *et al.* 2008 Sudden cardiac arrest associated with early repolarization. *N. Engl. J. Med.* **358**, 2016–2023. (doi:10.1056/NEJMoa071968)
25. Nam GB, Kim YH, Antzelevitch C. 2008 Augmentation of J waves and electrical storms in patients with early repolarization. *N. Engl. J. Med.* **358**, 2078–2079. (doi:10.1056/NEJMc0708182)
26. Rattanawong P *et al.* 2021 Does the age of sudden cardiac death in family members matter in Brugada syndrome? *J. Am. Heart Assoc.* **10**, e019788. (doi:10.1161/JAHA.120.019788)
27. Watanabe H *et al.* 2012 Clinical characteristics and risk of arrhythmia recurrences in patients with idiopathic ventricular fibrillation associated with early repolarization. *Int. J. Cardiol.* **159**, 238–240. (doi:10.1016/j.ijcard.2012.05.091)
28. Haissaguerre M *et al.* 2009 Characteristics of recurrent ventricular fibrillation associated with inferolateral early repolarization role of drug therapy. *J. Am. Coll. Cardiol.* **53**, 612–619. (doi:10.1016/j.jacc.2008.10.044)
29. Chen Y *et al.* 2017 Novel trigenic CACNA1C/DES/MYPN mutations in a family of hypertrophic cardiomyopathy with early repolarization and short QT syndrome. *J. Transl. Med.* **15**, 78. (doi:10.1186/s12967-017-1180-1)
30. Sun Z *et al.* 2004 Role of a KCNH2 polymorphism (R1047 L) in dofetilide-induced torsades de pointes. *J. Mol. Cell. Cardiol.* **37**, 1031–1039. (doi:10.1016/j.yjmcc.2004.09.001)
31. Calo L *et al.* 2016 A new electrocardiographic marker of sudden death in Brugada syndrome: the S-wave in lead I. *J. Am. Coll. Cardiol.* **67**, 1427–1440. (doi:10.1016/j.jacc.2016.01.024)
32. Antzelevitch C. 2006 Brugada syndrome. *Pacing Clin. Electrophysiol.* **29**, 1130–1159. (doi:10.1111/j.1540-8159.2006.00507.x)
33. Belhassen B, Glick A, Viskin S. 2004 Efficacy of quinidine in high-risk patients with Brugada syndrome. *Circulation* **110**, 1731–1737. (doi:10.1161/01.CIR.0000143159.30585.90)
34. Andorin A *et al.* 2017 The QUIDAM study: hydroquinidine therapy for the management of Brugada syndrome patients at high arrhythmic risk. *Heart Rhythm.* **14**, 1147–1154. (doi:10.1016/j.hrthm.2017.04.019)
35. Viskin S, Wilde AA, Krahn AD, Zipes DP. 2013 Inaccessibility to quinidine therapy is about to get worse. *J. Am. Coll. Cardiol.* **62**, 355. (doi:10.1016/j.jacc.2013.04.009)
36. Watanabe A *et al.* 2006 Low-dose isoproterenol for repetitive ventricular arrhythmia in patients with Brugada syndrome. *Eur. Heart J.* **27**, 1579–1583. (doi:10.1093/eurheartj/ehl060)
37. Shinohara T *et al.* 2014 Combination therapy of cilostazol and bepridil suppresses recurrent ventricular fibrillation related to J-wave syndromes. *Heart Rhythm.* **11**, 1441–1445. (doi:10.1016/j.hrthm.2014.05.001)
38. Hasegawa K *et al.* 2014 Long-term pharmacological therapy of Brugada syndrome: is J-wave attenuation a marker of drug efficacy? *Intern. Med.* **53**, 1523–1526. (doi:10.2169/internalmedicine.53.1829)
39. Koncz I *et al.* 2014 Mechanisms underlying the development of the electrocardiographic and arrhythmic manifestations of early repolarization syndrome. *J. Mol. Cell. Cardiol.* **68**, 20–28. (doi:10.1016/j.yjmcc.2013.12.012)
40. Ye D *et al.* 2022 Acacetin, a potent transient outward current blocker, may be a novel therapeutic for KCND3-encoded Kv4.3 gain-of-function-associated. *Circ. Genom. Precis. Med.* **15**, e003238.
41. Gurnett CA, De Waard M, Campbell KP. 1996 Dual function of the voltage-dependent Ca^{2+} channel alpha 2 delta subunit in current stimulation and subunit interaction. *Neuron* **16**, 431–440. (doi:10.1016/S0896-6273(00) 80061-6)
42. Fukuyama M *et al.* 2013 L-type calcium channel mutations in Japanese patients with inherited arrhythmias. *Circ. J.* **77**, 1799–1806. (doi:10.1253/circj.CJ-12-1457)